Wavelength and duration tunable soliton generation from a regeneratively mode-locked fiber laser

Bin Tan (谈 斌), Zhiyong Li (李智勇), Zhaoying Wang (王肇颖), Chunfeng Ge (葛春风), Dongfang Jia (贾东方), Wenjun Ni (倪文俊), and Shichen Li (李世忱)

Optoelectronic Information Science and Technology Lab, College of Precision Instrument and Optoelectronics Engineering, Tianjin University, Tianjin 300072

Received June 21, 2004

A 10-GHz soliton source with pulse duration between 4–8 ps and wavelength continuously tunable from 1530 to 1563 nm is presented. Using regeneratively mode-locking technology, the harmonically mode-locked fiber ring laser could work without pulse dropout at room temperature when no cavity length or polarization maintaining mechanism is available. Applying only one 980-nm laser diode pump, the average output power reaches more than 4 mW.

OCIS codes: 140.3510, 140.4050, 140.3600, 060.2410.

Optical short pulse source with high repetition rate is essential for ultra-high speed optical communication. This could be realized by external modulation of a continuous wave from distributed feedback Bragg (DFB) laser using an electroabsorption modulator (EAM)[1,2] or by exploiting a mode-locked laser diode (LD)[3]. However, pulses from such an EAM are with intrinsic chirp and the waveform and spectrum are not clear. Moreover the output is seriously limited when a proper bias voltage is set to achieve small duty cycle. The output of mode-locked LD, though stable and nearly transform limited, is wavelength untunable and power limited. In contrast, an actively and harmonically mode-locked fiber laser is favored for its tunable wavelength, short pulse duration, high repetition rate, and high output power.

This paper demonstrates a 10-GHz regeneratively mode-locked fiber laser (RMLFL) applying electrical phase locking technology[4,5]. Particularly the regenerative circuit is composed of commercial radio frequency (RF) components. With this technology, stable soliton stream with pulse duration tunable between 4–8 ps is achieved. No pulse dropout is observed at room temperature without any cavity length or polarization maintaining mechanism. The supermode noise is suppressed through cooperation of self phase modulation (SPM) and spectral filtering mechanism[6]. The usage of a tunable thin-film filter inside cavity makes the output wavelength continuously tunable from 1530 to 1563 nm. Only one 980-nm LD is used as pump in the laser and the average power could be higher than 4 mW. Such a RMLFL is efficient in high speed optical communication experiments[7,8] or supercontinuum generation application[9].

The experimental setup for the RMLFL is shown in Fig. 1. The optical cavity consists of 2.7-m Er^{3+}-doped fiber (EDF) pumped by a 980-nm LD, a wavelength division multiplexing (WDM) coupler, two isolators (ISO1, ISO2), 100-m dispersion shifted fiber (DSF), a thin film filter (TFF), an 80:20 coupler, a polarization controller (PC), and a $LiNbO_3$ modulator. The TFF is tunable from 1530 to 1560 nm with a bandwidth of 2 nm. The bias voltage of the modulator is set on the negative slope of the transfer function. The 20% port of the 20:80 coupler is connected to a 10:90 coupler, where the 10% port is for regeneration input and the 90% port for output. The parameters of output are simultaneously measured by a digital communication analyzer (DCA), an optical spectrum analyzer (OSA), and a second harmonic generation (SHG) autocorrelator through the connection of two 50:50 couplers. An optical amplifier (OA) is used to improve the power for SHG. The regeneration loop includes an O/E conversion module, a bandpass filter (BPF), a clock recovery unit (CRU), a phase shifter (PS), a directional coupler (DC), and a modulator driver (RF driver). Here the O/E module integrates a 10-GHz PIN and preamplifier together. The central frequency and bandwidth of BPF are 9.95 GHz and 50 MHz, respectively. The CRU is essentially a phase-locked loop and is able to recover clock signal from degraded data between 9.5 and 10.5 Gb/s. Some portion of the recovered clock is bypassed through the DC for online monitor and trigger use. The RF driver has 13-dB gain and 23-dBm saturated output at 10-GHz frequency.

When the RMLFL is set to work, the harmonic modes around 10 GHz are detected by the O/E module. Since the modes outside the bandwidth of BPF are blocked, the input of CRU is a narrow band signal. The recovered clock signal from CRU will be of a proper frequency

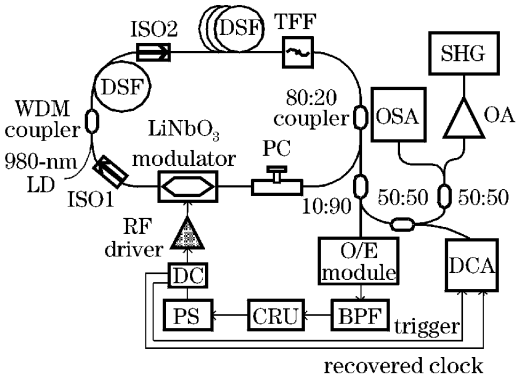

Fig. 1. Experimental setup of the RMLFL.

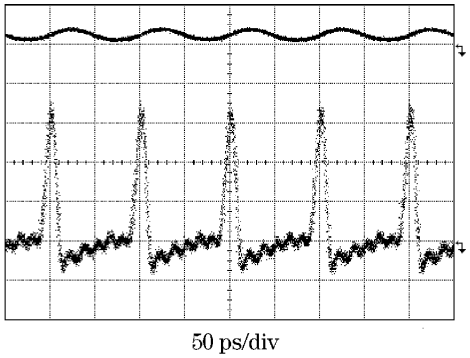

Fig. 2. Waveforms of optical pulses and recovered clock obtained from a DCA.

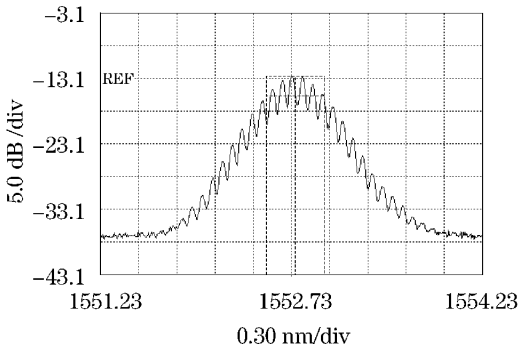

Fig. 3. Spectrum of output with 0.05-nm resolution.

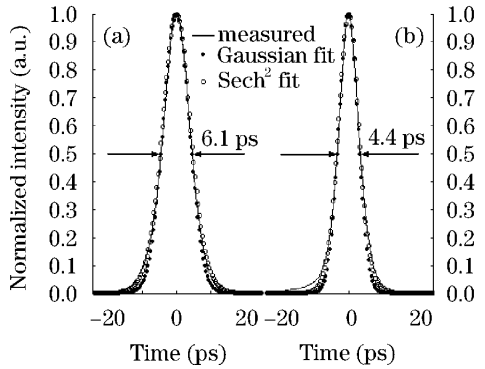

Fig. 4. Autocorrelation traces of measured (solid), Gaussian (points), and Sech^2 (circles) assumption.

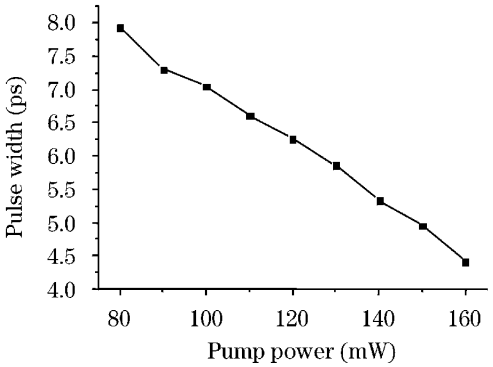

Fig. 5. Changes in pulse width against pump power.

up to the CRU's input. Such a clock signal is amplified and applied to the modulator by the RF driver, which excites or strengthens the proper frequency mode inside cavity. Certainly the enhanced mode will be redetected and reamplified through regenerative loop. After multiple roundtrips, the positive feedback mechanism finally leads to the stable mode-locking. In this experiment, the locked frequency is exactly 9.95 GHz. Typical waveforms of mode-locked pulses are shown in Fig. 2, which were obtained from the DCA with 40-GHz optical bandwidth and 50-GHz electrical bandwidth. The upper waveform stands for the recovered RF signal from one port of DC and the lower for mode-locked optical pulses. Both waveforms are clear and stable. The recovered clock is nearly a sine wave, which means only one mode is locked in the system. Figure 3 is the optical spectrum when the central wavelength of TFF is shifted to about 1553 nm and the pump power of the 980-nm LD is set to 120 mW, which is also clear and is in a shape of Sech^2.

To verify the intracavity soliton formation of RMLFL, autocorrelation traces of individual pulses are analyzed, which are shown in Fig. 4. Figure 4(a) is the case in accordance with Fig. 3, while Fig. 4(b) is the case with pump power of 160 mW. It is obvious that the autocorrelation traces (solid curves) are more fit with a Sech^2 profile (circles) than a Gaussian one (points). Considering the measured bandwidth of about 0.44 nm in case (a) and 0.583 nm in case (b), the time-bandwidth product (TBP) of the two pulses are calculated to be about 0.33 and 0.32 respectively, which could be thought as chirp-free soliton pulses. The measured relationship between pump power and pulse width also confirms the soliton characteristic. According to Fig. 5, the pulse width decreases smoothly as the pump power changes, which conforms to the well known soliton condition, where the pulse width is in inverse proportion to the average power[10]. The width could further decrease down if higher pump power is applied or the cavity loss is decreased.

Experimental results suggest that the RMLFL is able to operate stably between 1530−1563 nm. During the tuning process, the system keeps the mode-locking status and no polarization adjustment is required. The upper limit of output wavelength is only restricted by the TFF since no evident temporal or spectral degeneration is observed in this edge. In contrast, the RMLFL behaves poorer at wavelength shorter than 1530 nm due to the steep slope of EDF gain curve in this area. Figure 6 shows the dependences of pulse width and TBP on wavelength when pump power is set to 120 mW. In this figure, pulse width keeps increasing as the wavelength is tuned from 1530 to 1560 nm and the increase is remarkable between 1530 and 1540 nm. This phenomenon is caused by the negative slope of the EDF gain curve. In the current RMLFL configuration, the cavity loss is set to be large (~13 dB) and the system does not operate in deep gain saturation status. So the overall gain curve is wavelength discriminative and the power is dependent on wavelength. As a result, if the soliton condition is assumed[10], the pulse width scales up when the wavelength shifts from 1530 to 1560 nm. This also leads to the slightly asymmetric optical spectrum between 1530 and 1540 nm. However, the TBP transition from

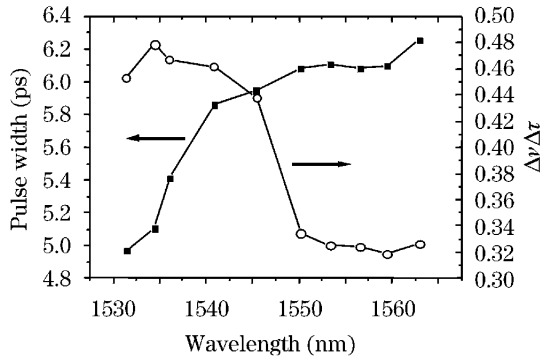

Fig. 6. Dependences of pulse width and TBP ($\Delta\nu\Delta\tau$) on wavelength.

1540 to 1550 nm is not consistent with the pulse width curve. Actually this is the transition of soliton solution to dispersion management soliton (DMS) transition induced by the dispersion sign change of DSF around 1550 nm. Rather than a traditional Sech^2 pulse, the DMS could be chirped or like a Gaussian shape[11]. Such a dispersion management condition is matched by pigtails of components and DSF inside cavity. The TBP (0.44−0.48) between 1530 and 1545 nm reveals the Gaussian characteristic of pulses. When the wavelength is longer than 1550 nm, pulse evolves into traditional soliton, which is also confirmed by the TBP (0.32−0.33) of this region.

Throughout the experiments, no pulse dropout is observed. At room temperature, the laser could work with both wavelength and duration ajustable at C-band. The average power of output could be higher than 4-mW using only one 980-nm LD (150 mW). However, nonpolarization operation and no bias control for the modulator may result in power fluctuation and increased timing jitter at last.

In conclusion, a stable RMLFL working at 10 GHz and wavelength tunable between 1530−1563 nm is achieved. Soliton pulses with duration between 4−8 ps and output reaching 4 mW could be generated directly from this laser. Such a source meets the requirements of optical time division multiplexing, high speed soliton transmission, pulse compression, and supercontinuum generation.

This work was supported by the National Natural Science Foundation of China (No. 60477022) and the Project of Tianjin United Institute of Optoelectronics (No. 033800411). B. Tan's e-mail address is tanmc@263.net.

References

1. K. Wakita, K. Yoshino, A. Hirano, S. Kondo, and Y. Noguchi, in *10th Intern. Conf. Indium Phosphide and Related Materials* thp-42, 679 (1998).
2. S. Oshiba, K. Nakamura, and H. Horikawa, IEEE J. Quantum Electron. **34,** 277 (1998).
3. H. Murai, H. T. Yamada, K. Fujii, Y. Ozeki, I. Ogura, T. Ono, and H. Yokoyama, in *Proceedings of ECOC'01* Tu.L.2.1, 180 (2001).
4. M. Nakazawa, E. Yoshida, and Y. Kimura, Electron. Lett. **30,** 1603 (1994).
5. E. Yoshida, N. Shimizu, and M. Nakazawa, IEEE Photon. Technol. Lett. **11,** 1587 (1999).
6. M. Nakazawa, K. Tamura, and E. Yoshida, Electron. Lett. **32,** 461 (1996).
7. T. Yamamoto, E. Yoshida, K. R. Tamura, K. Yonenaga, and M. Nakazawa, IEEE Photon. Technol. Lett. **12,** 353 (2000).
8. M. Nakazawa T. Yamamoto, and K. Tamura, Electron. Lett. **36,** 2027 (2000).
9. K. Mori, H. Takara, S. Kawanishi, M. Saruwatari, and T. Morioka, Electron. Lett. **33,** 1806 (1997).
10. G. P. Agrawal, *Nonlinear Fiber Optics, Third Edition & Application of Nonlinear Fiber Optics* (in Chinese) D. F. Jia, Z. H. Yu, B. Tan, Z. Y. Hu, and S. C. Li, (trans.) (Publishing House of Electronics Industry, Beijing, 2002) p. 97.
11. N. J. Smith, N. J. Doran, W. Forysiak, and F. M. Knox, J. Lightwave Technol. **15,** 1808 (1997).